Laser cladding as a flexible exploration tool for the design of cobalt-free hardfacing coatings made of high entropy materials

Clément Vary, Pascal Aubry, Ivan Guillot, Peter Grünc, Jörg Kasparc, Maria Barbosa

Available online at www.sciencedirect.com

ScienceDirect

Procedia CIRP 111 (2022) 201–204

www.elsevier.com/locate/procedia

12th CIRP Conference on Photonic Technologies [LANE 2022], 4-8 September 2022, Fürth, Germany

Laser cladding as a flexible exploration tool for the design of cobalt-free hardfacing coatings made of high entropy materials

Clément Vary[a,b]*, Pascal Aubry[a], Ivan Guillot[b], Peter Grün[c], Jörg Kaspar[c], Maria Barbosa[c]

[a] *Service d'Etudes Analytiques et de Réactivité des Surfaces (SEARS), CEA, Université Paris-Saclay, F-91191, Gif-sur-Yvette, France*
[b] *Université Paris-Est Créteil, ICMPE (UMR 7182), CNRS, F-94320 Thiais, France*
[c] *Fraunhofer Institute for Material and Beam Technology IWS, Dresden, Germany*

* Corresponding author. Tel.: +33-169-084-766; *E-mail address:* clement.vary@cea.fr

Abstract

Significant research efforts have been undertaken over the past forty years to replace the Stellite™ cobalt-based alloys, which boast outstanding performances when used as hardfacing coatings, but proved problematic especially in radioactive environments. This work's purpose is to contribute to this effort by coming up with viable substitutes made of Complex Concentrated Alloys (CCAs). Previous work evidenced the $(CrFeNi)_{90}Mo_5Ti_5$ alloy as a promising base that relies on the formation of intermetallic phases within a ductile matrix for an increase in hardness and an improved tribological behaviour. In this particular framework, the *in situ* alloying capabilities of the DED (Direct Energy Deposition) process were used for further explorations around this composition. Compositionally graded samples were successfully made despite the especially high brittleness of the alloys of interest. Coupled with an extensive use of the CALPHAD method, this combinatorial strategy dramatically speeds up material development compared to what the more conventional ways can achieve. The present paper emphasizes on the methodology and the high-throughput tools that were developed and used in this study, as such elements are growing in importance in the current context of intensive global research for new materials, especially in the CCAs field.

Keywords: Complex Concentrated Alloys; Direct Energy Deposition; CALPHAD method; hardfacing coatings; combinatorial metallurgy

1. Introduction

1.1. Applicative context

Many industrial systems involve metallic parts that may be put in sliding contact against each other, which often damages them at unacceptable rates if nothing is done. A common solution to this problem is to protect said moving metallic parts by coatings made of harder and more durable materials. The cobalt-based alloys regrouped under the Stellite™ designation (Deloro Inc.) are among the most widespread, as they have been providing the most consistent performances. However, cobalt has become either undesirable and/or too expensive for many applications, which tends to orient research toward the development of new cobalt-free materials. As far as hardfacing coatings are concerned, these substitute alloys are mostly nickel- or iron-based but none of them exhibits the same level of all-round performances as Stellites™.

The present paper covers some of the results included in ongoing investigations considering high-entropy materials as potential new entries in the cobalt-free hardfacing alloys catalogue.

1.2. High-entropy materials

This alloying concept was introduced simultaneously –but separately– by Yeh *et al.* [1] and Cantor *et al.* [2] in 2004. The general idea could be summed up as a will to explore the central parts of multi-elements phase diagrams, where there is no more distinction between principal and secondary elements. In these so-called high entropy alloys (HEAs), high values of the

10.1016/j.procir.2022.08.047

configurational entropy lead to the formation of single-phase microstructures to a much higher extent than anticipated, for broad compositional ranges across several systems [3,4]. Despite some of them displaying interesting properties [5], single-phase HEAs rarely reach the required industrial levels of performance and reliability. The research scope thus expanded itself to also include multi-phase microstructures, and the HEA label is now sometimes replaced by less specific acronyms, such as MPEAs (Multi-Principal Elements Alloys) or CCAs (Compositionally Complex Alloys or Complex Concentrated Alloys) [6].

Dealing with an almost infinite choice of compositions to explore can prove quite challenging, but with the CALPHAD method as a predictive tool and Direct Energy Deposition as a rapid manufacturing process, this difficulty may be overcome.

In direct continuation with previous work [7], the same alloying strategy is pursued. Introducing high –and easily adjustable– amounts of intermetallic phases within a more ductile matrix is prospected to display satisfying performance. The results obtained by Huser [7] have already narrowed down the possibilities to a promising alloy composition from the CrFeNiMoTi system: $(CrFeNi)_{90}Mo_5Ti_5$ (at%). The following section describes the strategy and the tools that were used to further refine this composition and its properties. The first steps consist in evaluating the influence of Cr, Fe and Ni on the microstructure, via both digital and experimental rapid screening strategies.

2. Tools and methodology

2.1. The CALPHAD method

In this study, the use of CALculated PHase Diagrams allowed to thoroughly explore the CrFeNiMoTi system, mostly in terms of phase fraction distribution across the compositional space. To do so, massive equilibrium calculations were performed using Thermo-Calc®'s batch mode and the TCHEA4 database. Equilibrium was computed at 1000K for all alloy compositions of the following structure: $Cr_vFe_wNi_xMo_yTi_z$, with {v,w,x,y,z} each ranging from 0 to 100 at% with a 5at% step, which represents 10,626 compositions. The phase fractions values were then extracted and rearranged using a specific representation. Other examples of this type of representation in different contexts can be found in [3] and [9].

2.2. Direct Energy Deposition (DED)

This additive manufacturing technique is a fast and flexible process and, despite all the challenges still associated to it to this day [10], it holds great potential in both industrial and research applications. In this framework, its use is particularly justified not only because of its ability to deposit hardfacing coatings, but also because of the possibility of *in situ* alloying during the fabrication process, through the simultaneous use of several powder feeders. This has already been identified in the literature as a very promising way of exploring HEA systems [7], [11–13].

Samples were therefore built in the form of compositionally graded walls where the content of Cr, Fe or Ni was set to vary between 15 and 40 at% by a 5at% step, with the other two elements acting as the balance. As illustrated in Figure 1, the aim is to manufacture "all-in-one" samples that provide enough material to run all the required tests on, while minimizing both the number of samples and the amount of raw materials used to make them.

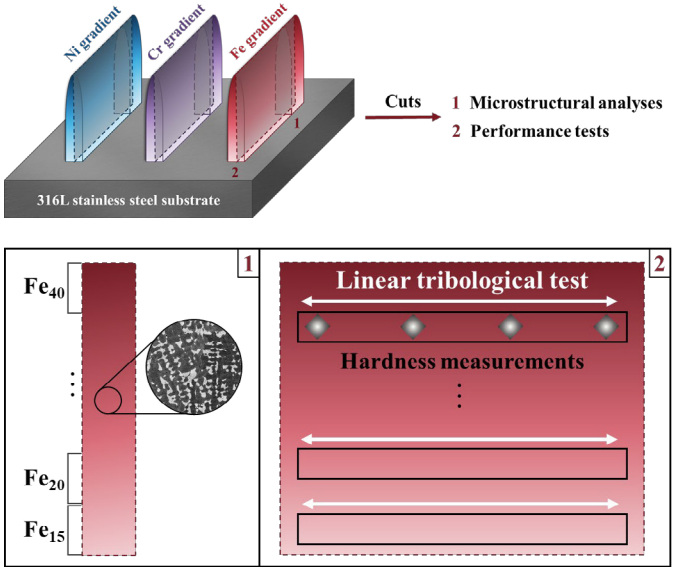

Fig. 1. Schematic description of the compositionally graded samples of this study and their purpose.

Such samples were manufactured according to two plans of experiments (Series 1&2) and on different DED machines, which offers a wider range of parameters and helps assessing feasibility when cladding with unknown alloys.

- Series 1: as described in Figure 1, graded walls containing six compositions each were made using an Optomec LENS™ DED machine (3kW IPG Photonics laser, λ=1070 nm, 400 µm fiber core). The parameters were set as follows: 600W laser power, 1.2mm laser spot size, 300mm/min feed rate and 10g/min powder flow rate. Six layers are stacked for each composition and the substrates' temperature was maintained at 700°C throughout the fabrication to hinder the formation of cracks.
- Series 2: the gradient for each element was split into two walls to keep the same wall dimensions, because of the much higher cladding tracks size. For each metal M (Cr, Fe or Ni), one wall contains the M_{15}, M_{20}, and M_{25} compositions, the other M_{30}, M_{35} and M_{40}. Four layers were dedicated to each composition. The laser used is a 4kW Laserline diode (λ=980 nm, 1mm fiber core) and the parameters were set as follows: 2080W laser power, 5mm laser spot size, 550mm/min feed rate and 26g/min powder flow rate. The substrates were preheated at 400°C.

These experiments were carried out in argon-filled fabrication chambers and using highly spherical powders with a 50-150µm granulometry. At this stage of the experimental campaign, the attention is mostly focused on feasibility and parameters optimization, as the alloys of interest are

particularly hard and brittle. Porosity control is also a challenge because of the overlapping melting and boiling temperatures between some elements/species.

Prior to this, preliminary work that consisted in the fabrication of five individual samples had been carried out. The compositions listed in Table 1 were chosen to expand the amount of first-hand experimental data, in areas of the compositional space where inaccuracies in the CALPHAD predictions were suspected.

Table 1. Compositions of alloys A to E (at%)

Alloy	Cr	Fe	Ni	Mo	Ti
A	18	36	36	5	5
B	25	25	40	5	5
C	37.5	15	37.5	5	5
D	35	20	35	5	5
E	32.5	25	32.5	5	5

Samples were obtained from the melting of elemental powders blends in alumina crucibles via the DED machine's laser (1.5kW laser power maintained for 15s), which ensures a slower cooling and a final microstructure closer to equilibrium.

All samples (Series 1&2 + alloys A to E) were cut, embedded and prepared for metallurgical analyses: SiC paper grinding (grades 220 to 2400), 3min of polishing in diamond suspensions (3µm and 1µm), and 3h spent vibrating in a silica suspension for final polishing and superficial stress relief. SEM observations for microstructural investigations (EBSD, EDS, BSE and SE pictures) were then performed on Tescan and Jeol SEM models both coupled with Bruker's Esprit software. The following operations were additionally performed on samples A to E:

- Vickers micro-hardness measurements: 20 indents were made at 2 kgf for 15s on a Clemex hardness tester and measured manually.
- XRD experiments, on a PanAnalytical X'Pert Pro instrument using a Co anode as the X-Ray source ($K_{\alpha 1}$ ray, λ=0.179 nm).

3. Results and discussions

3.1. CALPHAD results

The results were plotted for each phase, using tiled representations such as the one detailed in Figure 2 for the sigma phase.

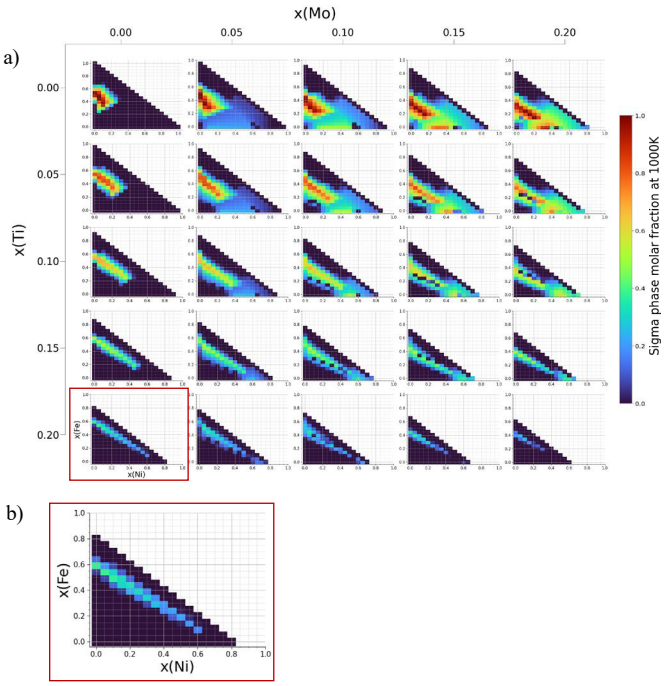

Fig. 2. a) Distribution of the sigma phase's molar fraction for compositions containing 20at% or less of Mo and Ti. b) Close-up view of the Mo_0Ti_{20} subplot.

These cartographies help visualizing trends in the influence of each element on the formation of phases across the compositional space. As the alloy design process advances, they are used to redirect the compositional choices depending on the experimental feedback.

3.2. Experimental results

3.2.1. Laser-melted powder blends

The hardness results, along with the experimental phase fractions values obtained from BSE pictures taken on alloys A to E, are compiled in Table 2.

Table 2. Mechanical and microstructural features of alloys A to E

		A	B	C	D	E
Vickers hardness (HV)		161±11	178±6	285±12	284±12	261±11
Phase fractions (vol%)	FCC	100	100	79.9	77.5	80.4
	Sigma	-	-	20.1	22.5	19.6

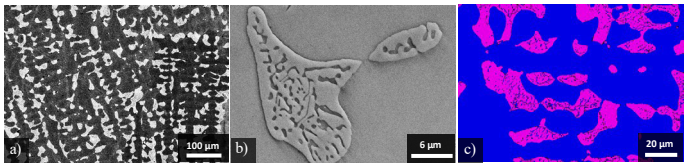

Fig. 3. Typical microstructures obtained in alloys C, D and E,: (a) BSE x200, FCC and sigma respectively in dark and bright contrast (sample E), (b) SE x4000, zoom on an FCC-constellated sigma nodule (sample E) and (c) EBSD mapping showing the FCC (blue) and sigma (pink) phases (sample D).

According to these observations and the XRD results, not only are all the phases fractions far from the computed values, but the Ni_3Ti and BCC phases were not even detected at all,

despite being predicted by the simulations in non-negligible amounts (~20-25 mol% each). The presence of the sigma phase was also strongly underestimated, resulting in low hardness values that do not come close to the 400-500 HV targeted range.

3.2.2. DED-made samples

The walls obtained both in series 1 and 2 are roughly 4cm long, 3cm high and 1cm wide, the ones made with a smaller laser spot (series 1) presenting a more regular shape. The examples shown in Figure 4 and 5 are both Fe gradients.

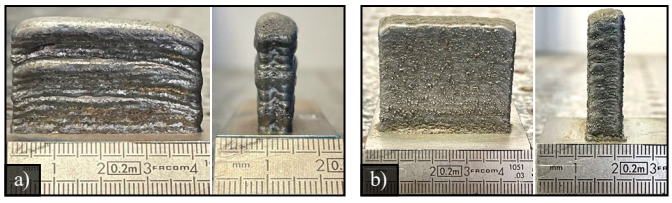

Fig. 4. visual appearance of the a) $Fe_{15\rightarrow25}$ (series 2) and b) $Fe_{15\rightarrow40}$ (series 1) DED-made walls

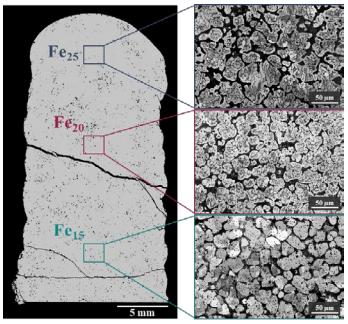

Fig. 5. Example of microstructural analyses performed on the $Fe_{15\rightarrow25}$ wall. The sigma and FCC phases appear respectively in bright and dark contrast on the BSE pictures.

Compared to samples A to E, the sigma phase content is much higher in these DED-made samples, and so are their hardness and brittleness. Cracks appear during either fabrication, cutting or even embedding of the samples, also because of internal residual stresses. Though they do not interfere with observations, they could cause problems during the tribological tests. Adjustments in the substrate heating conditions –before and during the fabrications– could be considered, along with stress relief post-treatments, to help decreasing crack occurrence.

The samples issued from series 1 display different microstructures: in the Fe gradient, the sigma phase presents more of a dendritic solidification pattern, similar to Figure 3 a). The complete observation results and comparisons with series 2 will allow to evaluate the influence of the process, independently of the chemical composition.

4. Conclusion and perspectives

In this paper, the starting points of an extensive exploratory work about the CrFeNiMoTi system were presented. Specific tools were developed for the systematic analyses of massive CALPHAD calculations. Some preliminary experimental results highlighted the limits of the TCHEA4 database for this particular system. Coupled with the high cooling rates inherent to DED, these inaccuracies make the thermodynamic predictions more difficult to interpret, but they can still be used to assess the influence of individual elements over broad compositional ranges.

Compositionally graded walls were made within a short timespan thanks to the *in situ* alloying capabilities of DED, accounting for 15 different alloy compositions. Hardness and tribology tests will eventually discriminate the alloys between them, but feasibility will also be an important factor, since hardfacing coatings are meant to be directly functional after deposition. The high hardness and brittleness observed in most samples suggest that the sigma phase content will have to be toned down. Overall, compositional adjustments will keep being made using the methodology presented here, until satisfying levels of performance are reached.

Acknowledgements

This work is part of the CladHEA+ project, an M-ERA.NET European project, in cooperation with FhG/IWS (Germany, project leader), NMTP (Russia), along with CEA and CNRS (France). The authors would like to thank the French National Research Agency (ANR) for their funding, along with Dr. Maria Barbosa, the CladHEA+ project leader from FhG/IWS.

References

[1] J.-W. Yeh *et al.*, 'Nanostructured High-Entropy Alloys with Multiple Principal Elements: Novel Alloy Design Concepts and Outcomes', *Adv. Eng. Mater.*, vol. 6, no. 5, Art. no. 5, 2004, doi: 10.1002/adem.200300567.

[2] B. Cantor *et al.*, 'Microstructural development in equiatomic multicomponent alloys', *Mater. Sci. Eng. A*, vol. 375–377, no. Supplement C, Art. no. Supplement C, 2004, doi: 10.1016/j.msea.2003.10.257.

[3] G. Bracq *et al.*, 'The fcc solid solution stability in the Co-Cr-Fe-Mn-Ni multi-component system', *Acta Mater.*, vol. 128, pp. 327–336, 2017, doi: 10.1016/j.actamat.2017.02.017.

[4] O. N. Senkov *et al.*, 'Refractory high-entropy alloys', *Intermetallics*, vol. 18, no. 9, Art. no. 9, 2010, doi: 10.1016/j.intermet.2010.05.014.

[5] Y. Zhang *et al.*, 'Microstructures and properties of high-entropy alloys', *Prog. Mater. Sci.*, vol. 61, no. Supplement C, Art. no. Supplement C, 2014, doi: 10.1016/j.pmatsci.2013.10.001.

[6] D. B. Miracle and O. N. Senkov, 'A critical review of high entropy alloys and related concepts', *Acta Mater.*, vol. 122, no. Supplement C, Art. no. Supplement C, 2017, doi: 10.1016/j.actamat.2016.08.081.

[7] G. Huser *et al.*, 'Study of the elaboration of high entropy material from powder by laser additive manufacturing', *Procedia CIRP*, vol. 94, pp. 270–275, 2020, doi: 10.1016/j.procir.2020.09.051.

[8] D. Boisselier and S. Sankaré, 'Influence of Powder Characteristics in Laser Direct Metal Deposition of SS316L for Metallic Parts Manufacturing', *Phys. Procedia*, vol. 39, pp. 455–463, 2012, doi: 10.1016/j.phpro.2012.10.061.

[9] T. Rieger *et al.*, 'Study of the FCC+L12 two-phase region in complex concentrated alloys based on the Al–Co–Cr–Fe–Ni–Ti system', *Materialia*, vol. 14, p. 100905, 2020, doi: 10.1016/j.mtla.2020.100905.

[10] N. Ahmed, 'Direct metal fabrication in rapid prototyping: A review', *J. Manuf. Process.*, vol. 42, pp. 167–191, 2019, doi: 10.1016/j.jmapro.2019.05.001.

[11] B. Gwalani *et al.*, 'Compositionally graded high entropy alloy with a strong front and ductile back', *Mater. Today Commun.*, vol. 20, p. 100602, 2019, doi: 10.1016/j.mtcomm.2019.100602.

[12] H. Dobbelstein *et al.*, 'Laser metal deposition of compositionally graded TiZrNbTa refractory high-entropy alloys using elemental powder blends', *Addit. Manuf.*, vol. 25, pp. 252–262, 2019, doi: 10.1016/j.addma.2018.10.042.

[13] H. Dobbelstein *et al.*, 'Laser metal deposition of refractory high-entropy alloys for high-throughput synthesis and structure-property characterization', *Int. J. Extreme Manuf.*, vol. 3, no. 1, p. 015201, 2021, doi: 10.1088/2631-7990/abcca8.